

Alma Mater Studiorum Università di Bologna
Archivio istituzionale della ricerca

Identification of polymer concrete damping properties

This is the final peer-reviewed author's accepted manuscript (postprint) of the following publication:

Published Version:

Troncosi, M., Canella, G., Vincenzi, N. (2022). Identification of polymer concrete damping properties. PROCEEDINGS OF THE INSTITUTION OF MECHANICAL ENGINEERS. PART C, JOURNAL OF MECHANICAL ENGINEERING SCIENCE, 236(21), 10657-10666 [10.1177/0954406220949587].

Availability:

This version is available at: <https://hdl.handle.net/11585/872192> since: 2022-10-09

Published:

DOI: <http://doi.org/10.1177/0954406220949587>

Terms of use:

Some rights reserved. The terms and conditions for the reuse of this version of the manuscript are specified in the publishing policy. For all terms of use and more information see the publisher's website.

This item was downloaded from IRIS Università di Bologna (<https://cris.unibo.it/>).
When citing, please refer to the published version.

(Article begins on next page)

This is the final peer-reviewed accepted manuscript of:

IDENTIFICATION OF POLYMER CONCRETE DAMPING PROPERTIES

The final published version is available online at:
<https://journals.sagepub.com/doi/full/10.1177/0954406220949587>

Rights / License:

The terms and conditions for the reuse of this version of the manuscript are specified in the publishing policy. For all terms of use and more information see the publisher's website.

This item was downloaded from IRIS Università di Bologna (<https://cris.unibo.it/>)

When citing, please refer to the published version.

IDENTIFICATION OF POLYMER CONCRETE DAMPING PROPERTIES

Marco Troncossi^{1(*)}, Giulio Canella², Nicolò Vincenzi²

¹ University of Bologna, viale del Risorgimento 2, Bologna, IT 40136

² Bucci Industries, via Granarolo 167, Faenza, Ravenna, IT 48018

(*) Email: marco.troncossi@unibo.it

ABSTRACT

The damping properties of a commercial polymer concrete are the subject of this application-driven study, which is aimed to investigate the material suitability as a filler of machine bed components to limit vibrations arising in machine tools and automatic machines working at high dynamics. Two main goals are targeted: (i) quantitative evaluation of the elastodynamic effects due to the polymer concrete insertion into typical components of machine beds, in order to effectively assess its practical potential and (ii) determination of reliable models of the material, needed to simulate the dynamic response of new design solutions of machines featuring structural components filled with the polymer concrete. The paper is mainly focused on the methodological approach of both the experimental campaign and the signal processing that were carried out. Based on the promising results achieved, the possible use of the polymer concrete as a viable solution to enhance the dynamic behavior of an automatic machine is finally investigated and discussed as a case study.

Keywords: Vibration and Acoustics, Dynamic Modelling, Material Testing, Concrete, Dampers

1. INTRODUCTION

The accuracy of automatic machines and machine tools is known to be highly hampered by an uncontrolled elastodynamic behavior of the machine components. With a particular focus on machine tools, vibrations and chatter can be triggered by several sources in a wide bandwidth, e.g. by tool cutting forces and/or inertial loads associated with the rapid movements for spindle positioning, or even by external vibrations transmitted through the ground [1, 2]. If excessive, these vibrations can reduce the tool life, degrade the quality of the machined surfaces, and cause unacceptable tolerances of the final products. Limiting their effects is thus mandatory in high-performance machines [3]. One problem is that, just due to the variegated sources of vibrations and working conditions, moving the system natural frequencies out of the excitation bandwidth could be difficult or even impossible. The introduction of vibration absorbers or tuned mass dampers could optimize the system dynamics, but it might be unfeasible in practice due to unacceptable design complexity. Hence, an effective way to improve the dynamic stability of the machine could be using special materials for structural components [4]. Hybrid structures, e.g. including polymer concretes (also referred to as metal castings), metal foams or fiber reinforced composites, generally prove enhanced mechanical properties with respect to structures made of steel or cast iron only [4-9]. In particular, polymer concretes are mainly exploited due to their damping properties [5, 10-14]. Commonly added as filling material of metal structural components, the polymer concrete efficiently absorbs the dynamic load energy and can thus limit the amplitude of vibrations triggered by the machine operations. Therefore, it proves particularly suitable for beds of machine tools featuring high performance and high precision [4, 8, 15-18].

In this context, an experimental investigation was performed to accurately characterize the damping properties of a polymer concrete proposed as a damping filler of machine bed

components. The study is application-driven, oriented to a practical case study offered by an industrial partner, to state if and how a specific commercial polymer concrete is a viable solution to enhance the dynamic performance of an automatic machine produced by the company. In particular, a rigorous and repeatable methodology (to possibly investigate other materials) was required to provide quantitative results suitable (i) to evaluate the actual effectiveness of the material and (ii) to set reliable models of the material involved in analytical or numerical elastodynamic analyses. Specifically, realistic values of its damping parameters are necessary to properly predict the dynamic response of different design solutions of new machine architectures featuring the damping filler. An extensive experimental campaign was carried out, mainly consisting in impact tests performed on ad-hoc specimens. To achieve the first goal, comparative tests were performed on two metal beams, featuring a hollow cross section with and without, respectively, the core filled with the polymer concrete. Modal parameters and the free response of the beams to impact excitations were computed, analyzed, and compared from different perspectives (which are discussed) to bring the filler effects out. For the second target, experimental modal analyses were performed on three specimens, i.e. beams made of the polymer concrete only, featuring different stiffness. The aim was indeed to evaluate the modal parameters on a large bandwidth in order to extract experimental data suitable to set a material model as general as possible. Based on the experimental data, some alternative models of the material damping properties and the values of the corresponding parameters are proposed and discussed (focusing on their implementation in FEM software, largely used by manufacturer companies). To demonstrate the impact of the findings, the design process of a machine revised architecture, featuring concrete-filled bed components, is outlined and some preliminary results are discussed.

2. MATERIALS AND METHODS

2.1 Specimens

The preliminary choice of the company (based on market analysis, supply policy, and technical aspects, e.g. casting and filling processes) targeted the polymer concrete *EPUMENT 140/5*, a three component cast polymer based on an epoxy resin and produced by *RAMPF®*, as the object of investigation (Table 1). According to the test aims, two families of specimens were produced for the experimental campaign (Table 2): (i) two steel beams, with a rectangular hollow cross section (5 mm thick), one hollow and the other one filled with the polymer concrete (Fig. 1a), for the back-to-back testing conceived to measure the damping properties of the filler; (ii) polymer concrete beams with rectangular cross section featuring different size (Fig. 1b). In order to avoid outcome uncertainties due to the concrete composition, the three specimens considered in this study were obtained by cutting slices with different thickness from the same beam.

2.2 Experimental setup and test procedures

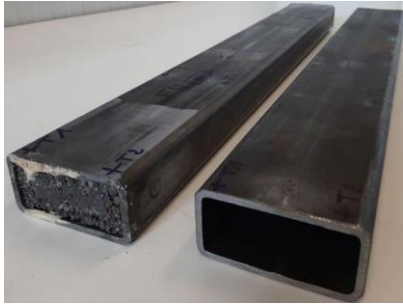
All the specimens were subjected to roving-hammer impact tests in free-free boundary condition to perform modal and free response analyses, in Frequency and Time domains, respectively. In practice, the beams were suspended by a low-stiffness elastic rope (Fig. 2a), instrumented with a tri-axial accelerometer placed at one corner (T1 in Fig. 2b), and excited with an impact hammer. The modal geometry consisted of 20 nodes that were excited along Y and Z directions (Fig. 2b), 10 times each for the sake of statistical reliability. Specimen *E03* is an exception, being represented by 10 nodes only, due to its small thickness. Acceleration and force signals were sampled at 8192Hz, for the duration of 4s.

Table 1: Nominal properties of *EPUMENT 140/5* (from commercial datasheet).

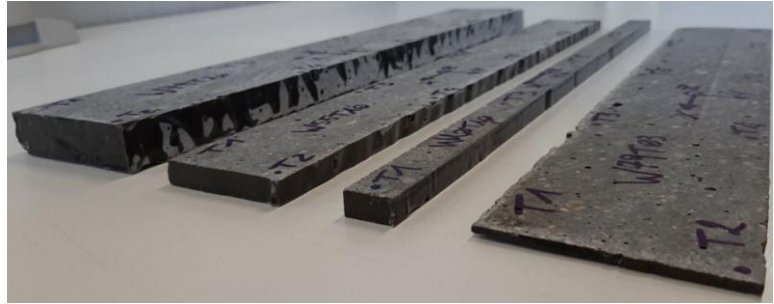
Density: ρ	2300 kg/m ³
Modulus of elasticity: E	> 30000 N/mm ²
Logarithmic decrement: δ	0.035
Wall thickness of cast: t_{min}	> 25 mm
Maximum grain size: ϕ	5 mm

Table 2: Specimen properties.

Name	Description	Size [mm]	Mass [kg]
<i>HSB</i>	Hollow steel beam	100x50x750	7.98
<i>FSB</i>	Steel beam filled with <i>EPUMENT 140/5</i>	100x50x750	13.88
<i>E40</i>	<i>EPUMENT 140/5</i> beam	79x40x500	3.66
<i>E20</i>	<i>EPUMENT 140/5</i> beam	79x20x500	1.82
<i>E03</i>	<i>EPUMENT 140/5</i> beam	79x3x500	0.27

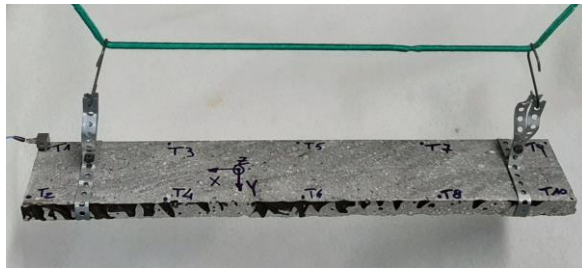


(a)

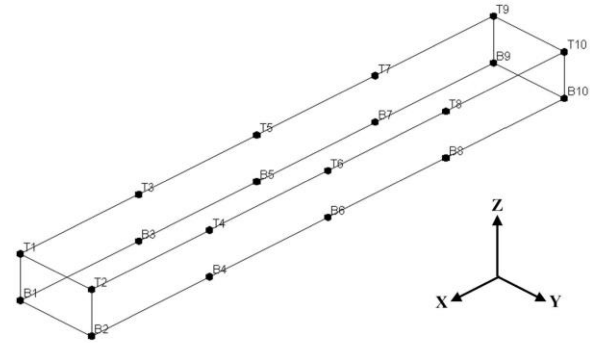


(b)

Figure 1. Test specimens: (a) concrete-filled and hollow steel beams; (b) polymer concrete beams.



(a)



(b)

Figure 2. (a) Example of test set up: specimen *E20*; (b) modal geometry of the beams.

2.3 Signal processing

It is known that structural damping is generally difficult to identify and even more difficult to model. In the field of Sound and Vibrations, the most popular way is the definition of damping coefficients in the Frequency domain. The literature offers a number of parameters, depending on the specific sector of application, which are associated with a single vibration mode, e.g. *damping ratio*, *logarithmic decrement*, *loss factor*, *quality factor*, *decay constant*... In practice, they carry very similar information, being interrelated through analytical formulations [19]. The datasheet of *EPUMENT 140/5* (Table 1) provides the logarithmic

decrement as a measure of its damping properties, but information relative to the test procedures for its determination are not known. In this study, the damping ratio (ζ , also known as *damping coefficient* or *fraction of critical damping*) is chosen as the target of the experimental investigation.

For all the tests, excitation and response signals were processed to compute the Frequency Response Functions (*FRFs*) and – by means of the so-called *POLYMAX* algorithm [20] – the modal parameters of the specimens, i.e. mode shapes X_i , natural frequencies ω_{ni} , and damping ratios ζ_i ($i = 1, 2, \dots$) [21].

Since the additional mass of the filler material is expected to lower the natural frequencies of specimen *FSB* with respect to *HSB*, the direct comparison of their damping ratios could be not comprehensive to practically assess the global dynamic effect associated with the introduction of the polymer concrete into the hollow section of the steel beams. Hence, the overall free damped responses of *HSB* and *FSB* were analyzed in Time domain, at first computing the time needed to reduce the overall vibration level by a certain factor. The idea is similar to the *reverberation time* concept used in Acoustics [22] and differs from the previously mentioned parameters by considering the overall vibration signal instead of single vibration modes. In particular, a scalar index (hereinafter named t_{95}^H and t_{95}^F for *HSB* and *FSB*, respectively) is calculated as the instant when the running average of the acceleration peaks drops to 5% of its maximum value. Such a metrics is representative of the structural damping properties of the specimen materials (steel and steel/*EPUMENT*) irrespective of the actual response amplitudes. The latter depend on both the resonance frequencies and the impact force energy, which resulted significantly different for the two specimens (cf. Section 3.1). Hence, to consider the specific behavior of the two beams as well, a further analysis is proposed aiming at the evaluation of the energy level ratio between the response (vibration) and the excitation (impact). In particular, for both the tested beams, the ratios ρ_{RMS}^H and ρ_{RMS}^F between the Root Mean Square (*RMS*) values of acceleration and impact force are computed (for the duration t_{95}^H and t_{95}^F , respectively) and compared.

Based on experimental data, a number of damping models could be derived, their choice depending on the intended use. The specific application-driven aim of this work led to target numerical models suitable to FEM simulations. Based on most FEM software specifications, three models are here determined (and discussed later) along with the corresponding parameter values:

1. proportional damping (*Model 1*);
2. constant damping ratio (*Model 2*);
3. piecewise-constant damping ratios (*Model 3*).

With reference to the free-vibration equations of motion in Eq. 1, the proportional damping model, also known as *Rayleigh model* [21, 23], assumes the viscous damping coefficients matrix \mathbf{C} as a linear combination of the mass and stiffness matrices, \mathbf{M} and \mathbf{K} respectively (Eq. 2). This mathematical expedient permits the diagonalization of all the matrices, largely simplifying the solution of the Eq. 3, thus explaining the wide spreading of this approach which, on the other side, has no physical justification and may even lead to inaccuracies [24].

$$\mathbf{M}\ddot{\mathbf{x}} + \mathbf{C}\dot{\mathbf{x}} + \mathbf{K}\mathbf{x} = \mathbf{0} \quad (1)$$

$$\mathbf{C} = \alpha\mathbf{M} + \beta\mathbf{K} \quad (2)$$

$$\mathbf{M}\ddot{\mathbf{x}} + (\alpha\mathbf{M} + \beta\mathbf{K})\dot{\mathbf{x}} + \mathbf{K}\mathbf{x} = \mathbf{0} \quad (3)$$

The proportional damping coefficients α and β can be estimated by means of spectral modelling [23]. For the i^{th} vibrational mode, under the assumption of proportional damping, the following expression holds:

$$2\zeta_i\omega_{ni} = \frac{c_i}{m_i} = \frac{\alpha m_i + \beta k_i}{m_i} = \alpha + \beta\omega_{ni}^2, \quad (4)$$

where m_i , k_i , c_i , are the modal mass, modal stiffness, and modal damping of the i^{th} mode, respectively. Once the modal parameters ω_{ni} and ζ_i are known for N modes, Eq. (5) directly provides the coefficients α and β :

$$\boldsymbol{\lambda} = (\mathbf{A}^T \mathbf{A})^{-1} \mathbf{A}^T \mathbf{b}, \quad (5)$$

with

$$\boldsymbol{\lambda} = \begin{bmatrix} \alpha \\ \beta \end{bmatrix}; \mathbf{A} = \begin{bmatrix} 1 & \omega_{n1}^2 \\ \vdots & \vdots \\ 1 & \omega_{nN}^2 \end{bmatrix}; \mathbf{b} = 2 \begin{bmatrix} \zeta_{n1}\omega_{n1} \\ \vdots \\ \zeta_{nN}\omega_{nN} \end{bmatrix}. \quad (6)$$

The higher the number modes N and the larger the frequency bandwidth $[\omega_{n1}, \omega_{nN}]$, the more general the resulting model. This is the reason why three beams featuring different mass and stiffness characteristics were produced and tested.

3. RESULTS

3.1 Evaluation of *EPUMENT 140/5* damping effectiveness

The back-to-back comparison between the hollow and concrete-filled steel beams (*HSB* and *FSB*, respectively) was conceived to assess the effects of the polymer concrete *EPUMENT 140/5* on the elastodynamic behavior of the specimen, with a special focus on its damping capability. Table 3 lists the modal parameters estimated through Experimental Modal Analysis (EMA) as well as their comparison, in terms of ratio of the specimens damping ratios and percentile variation of natural frequencies. It is noteworthy the high increment of the torsional mode natural frequencies due to the filler despite the general decrease of flexural mode resonances caused by additional mass. The mean values (μ) of damping ratios and their ratios are computed, along with the corresponding standard deviations (σ) and relative standard deviations ($\sigma^* = \sigma/\mu \cdot 100$). Notwithstanding the significant scatter of results (cf. σ^*), it can be reasonably concluded that *EPUMENT 140/5* proves good damping properties, being the damping ratios of *FSB* on the average about three times the *HSB* ones.

The Time domain analysis of the overall free response of the specimens was performed to consider simultaneously all the vibration modes excited by the impact force. For each impact tests performed on the two beams, the indices t_{95}^H , t_{95}^F and the ratios ρ_{RMS}^H , ρ_{RMS}^F were computed, respectively, as a measure of the vibration amplitude decay rates and of the energy dissipations due to structural damping. The results reported here refer to the acceleration Z component of point T1 (Fig. 2), $\ddot{\mathbf{z}}_{T1}$, in response to the impact force provided to the same point along Z , \mathbf{f}_{T1z} .

For t_{95} indices, the running average of peaks has been computed referring to moving windows with different widths, in order to check the results' sensitivity to this algorithm parameter. The scatter proves very small for windows containing from 5 to 40 points, the maximum

Table 3: Modal parameters of hollow (superscript H) and concrete-filled (F) steel beams.

Mode shape X_i	Mode order i		Natural Frequency ω_{ni} [Hz]		Damping ratio ζ_i [%]		Comparison FSB vs. HSB	
Description	HSB	FSB	ω_{ni}^H	ω_{ni}^F	ζ_i^H	ζ_i^F	ζ_i^F / ζ_i^H	$\Delta\omega_{ni}^{FH}$
1 st flexural mode (XZ plane)	1	1	602	506	0.09	0.26	3.04	-16.0%
1 st flexural mode (XY plane)	2	2	1030	887	0.06	0.13	2.33	-13.9%
1 st torsional mode (X axis)	3	4	1298	1584	0.05	0.25	5.40	+22.1%
2 nd flexural mode (XZ plane)	4	3	1414	1333	0.07	0.13	1.93	-5.7%
2 nd torsional mode (X axis)	5	7	1573	3161	0.05	0.22	4.62	+100.9%
3 rd flexural mode (XZ plane)	6	6	2148	2463	0.08	0.22	2.90	+14.6%
2 nd flexural mode (XY plane)	7	5	2474	2199	0.06	0.14	2.57	-11.1%
Mean (μ)					0.06	0.19	3.26	
Std. (σ)					0.015	0.058	1.272	
Rel. Std. (σ^*)					24.2%	29.6%	39.1%	

relative standard deviation associated with the obtained t_{95} values being $\sigma_{p5-40}^* = 3.06\%$. Considering moving windows containing 25 peak values, the main results (averaging the 10 test data for each specimen) confirm that the filler material introduced in the steel beam core triples the damping characteristics:

$$t_{95}^H = 0.358s \ (\sigma_{t1-10}^* = 6.19\%)$$

$$t_{95}^F = 0.119s \ (\sigma_{t1-10}^* = 5.87\%)$$

As an example, Fig. 3 reports the time signal responses of the specimens measured in single impact tests (third and fifth runs for HSB and FSB , respectively) and the running averages of 25 amplitude peaks (red curves).

It can also be noted the difference between the acceleration amplitude levels, which are not taken into account when comparing both the t_{95} indices and the damping ratios. What is more, in order to excite the FSB modes higher impact forces were required with respect to HSB (Fig. 4). The ratios between the RMS values of accelerations and impact forces (computed over time windows lasting 0.358s and 0.119s for HSB and FSB , respectively) make it intrinsically possible to account for this aspect too. The mean values, averaged over the 10 tests, and relative standard deviations are:

$$\rho_{RMS}^H = \frac{\ddot{z}_{T1_RMS}^H}{f_{T1z_RMS}^H} = 54.3 \ (\sigma_{t1-10}^* = 18.97\%) \quad \Rightarrow \quad \frac{\rho_{RMS}^H}{\rho_{RMS}^F} = 8.09.$$

$$\rho_{RMS}^F = \frac{\ddot{z}_{T1_RMS}^F}{f_{T1z_RMS}^F} = 6.1 \ (\sigma_{t1-10}^* = 3.39\%)$$

Their comparison stresses the influence of the polymer concrete core to a greater extent than the previous analyses and confirms once and for all the potential suitability of *EPUMENT 140/5* as a filler material of machine bed components to limit vibrations.

3.2 Material model

Form the EMA performed on the three polymer concrete specimens *E03*, *E20*, and *E40*, 24 pairs (ω_{ni} , ζ_i) were retrieved and exploited to determine the damping parameters of the material models to be used in numerical analyses (where filled components may be possibly made of material different from the steel of specimens HSB and FSB).

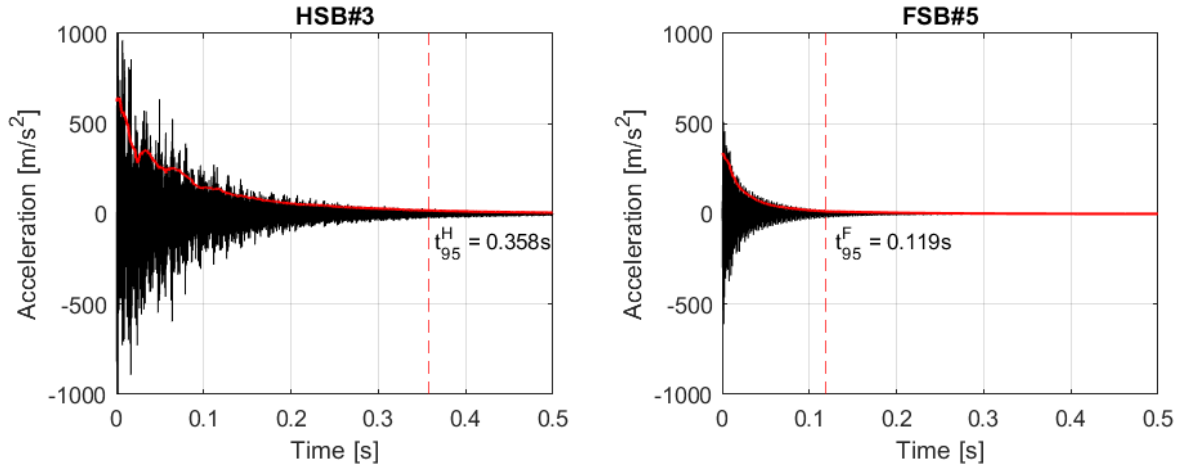


Figure 3. Examples of free responses of *HSB* and *FSB*.

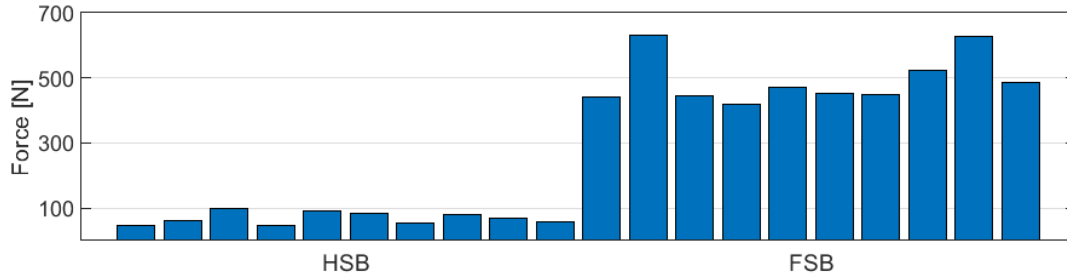


Figure 4. Peak values of the impact forces acting on point T1 in Z direction measured for all the tests.

Model 1 is here defined as the proportional damping model of Eqs. (1, 2), very popular in FEM software. Introducing the experimental data (ω_{ni}, ζ_i) into Eq. (6), Eq. (5) provides $\alpha = 46.27s^{-1}$ and $\beta = 5.88 \cdot 10^{-7}s$ which completely determine model (Fig. 5). It can be noticed that *Model 1* matches satisfactorily the experimental data only for the bandwidth higher than 500 Hz. Based on the application which the study is primarily addressed to, this could be a problem as the first natural frequencies of machine basements are generally below 100 Hz, where *Model 1* largely overestimates the material damping property, up to one order of magnitude. FEM simulations could thus provide unreliable (and not safe) results.

3.2 Material model

For the EMA performed on the three polymer concrete specimens *E03*, *E20*, and *E40*, 24 pairs (ω_{ni}, ζ_i) were retrieved and exploited to determine the damping parameters of the material models to be used in numerical analyses (where filled components may be possibly made of material different from the steel of specimens *HSB* and *FSB*).

Model 1 is here defined as the proportional damping model of Eqs. (1, 2), very popular in FEM software. Introducing the experimental data (ω_{ni}, ζ_i) into Eq. (6), Eq. (5) provides $\alpha = 46.27s^{-1}$ and $\beta = 5.88 \cdot 10^{-7}s$ which completely determine model (Fig. 5). It can be noticed that *Model 1* matches satisfactorily the experimental data only for the bandwidth higher than 500 Hz. Based on the application which the study is primarily addressed to, this could be a problem as the first natural frequencies of machine basements are generally below 100 Hz, where *Model 1* largely overestimates the material damping property, up to one order of magnitude. FEM simulations could thus provide unreliable (and not safe) results.

Hence, two models are proposed (available in most FEM software): constant and piecewise-constant damping ratios (*Model 2* and *Model 3*, respectively) are simply computed by averaging the experimental values within discrete frequency bandwidths (Fig. 6). Table 4

reports their values along with the measures of their scatter. The bandwidths defined for *Model 3* are chosen as those minimizing the relative standard deviations σ_i^* associated with the mean values $\bar{\zeta}_i$.

In the authors' analysis of results, *Model 2* ($\bar{\zeta} = 0.73\%$) is considered as the best choice for representing *EPUMENT 140/5* properties in numerical simulations, as it is the simplest one and proves suitable scatter with respect to experimental values ($\zeta_{\min}^{\text{exp}} = 0.46\%$, $\zeta_{\max}^{\text{exp}} = 0.99\%$) in the whole bandwidth of interest. Nonetheless, *Model 1* and *Model 3* have been presented here due to their underlying approach which could be more suitable for other materials.

It is worth noting that the logarithmic decrement computed from the damping ratio $\bar{\zeta}$ through the following equation [21, 23]

$$\bar{\delta} = \frac{2\pi\bar{\zeta}}{\sqrt{1-\bar{\zeta}^2}} = 0.046$$

is 30% larger than the nominal value reported in Table 1.

Since the material model is here supposed to be implemented in FEM software, the comparison between experimental and numerical modal analysis requires to update the values of density (ρ) and Modulus of elasticity (E) of Table 1 to $\bar{\rho} = 2292 \text{ kg/m}^3$ and $\bar{E} = 35196 \text{ MPa}$ in order to validate the numerical models. Table 5 reports, as an example referred to specimen *E40*, the better accuracy of the validated model (FEM2) with respect to the model (FEM1) obtained starting from the nominal value of Table 1.

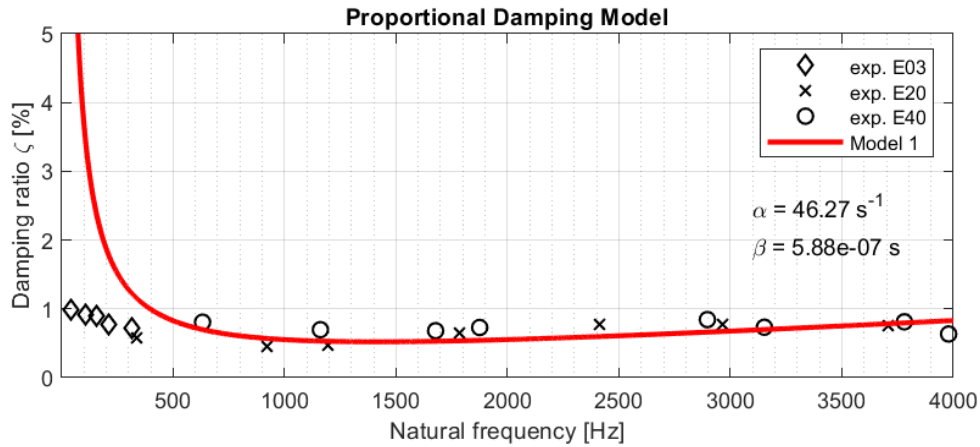


Figure 5. Experimental values of material damping ratios and their interpolation based on *Model 1*.

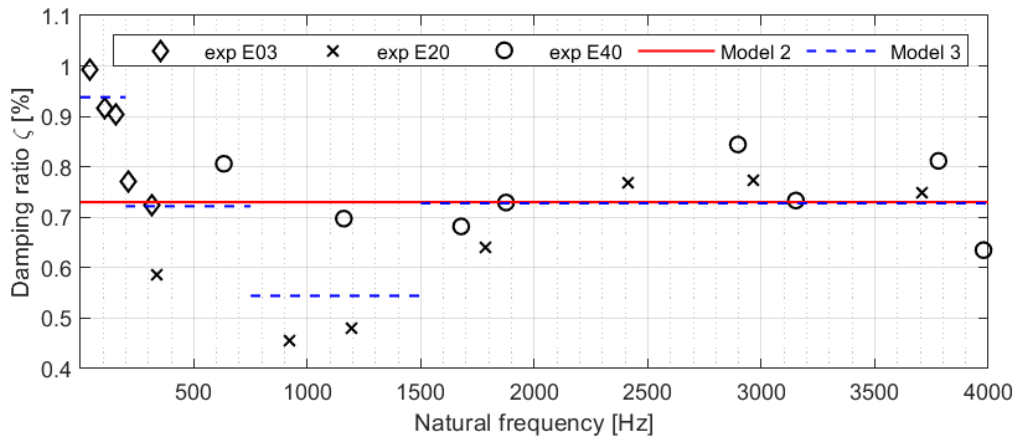


Figure 6. *Model 2*, *Model 3*, and experimental values of material damping ratios.

Table 4: Constant (*Model 2*) and piecewise-constant (*Model 3*) damping ratio models.

Bandwidth [Hz]	<i>Model 2</i>			<i>Model 3</i>		
	$\bar{\zeta}$ [%]	σ [%]	$\sigma^* = \sigma / \bar{\zeta}$	$\bar{\zeta}_i$ [%]	σ_i [%]	$\sigma_i^* = \sigma_i / \bar{\zeta}_i$
0-200	0.73	0.12	17.0%	0.94	0.05	5.2%
200-750				0.72	0.10	13.4%
750-1500				0.54	0.13	24.4%
≥ 1500				0.73	0.06	8.8%

Table 5: Natural frequencies of *E40*: experimental data (EMA), preliminary (FEM1), and validated (FEM2) numerical results.

Mode	EMA	FEM1		FEM2	
	ω_{ni} [Hz]	ω_{ni} [Hz]	$\Delta\omega_{ni}$	ω_{ni} [Hz]	$\Delta\omega_{ni}$
1 st flexural mode (XZ plane)	632	580	-8.2%	629	-0.5%
1 st flexural mode (XY plane)	1161	1059	-8.8%	1149	-1.0%
2 nd flexural mode (XZ plane)	1678	1540	-8.2%	1671	-0.4%
1 st torsional mode (X axis)	1875	1700	-9.3%	1844	-1.7%
2 nd flexural mode (XY plane)	2897	2609	-9.9%	2831	-2.3%
3 rd flexural mode (XZ plane)	3152	2876	-8.8%	3121	-1.0%
2 nd torsional mode (X axis)	3780	3407	-9.9%	3697	-2.2%
1 st torsional mode (X axis)	3979	3601	-9.5%	3907	-1.8%

4. APPLICATION: NEW DESIGN OF A MACHINE BED

The practical application of the previous findings turns out into the design of a new variant of an automatic machine bed. This Section illustrates the design approach, limited to the first steps, to complete the outline of the methodological framework which the paper is devoted to: details of the machine and the final outcome cannot be reported, being confidential information of the manufacturer.

The target of the investigation is the frame of an automatic machine that basically consists of a main basement which supports a beam structure hosting rotary operational units (Fig. 7a). In order to introduce the damping material filler, the current design of the structure is firstly revised by replacing folded steel sheet components with hollow cross section beams, welded or bolted to each other, still keeping the same overall layout. Five possible solutions, featuring different production complexity, are analyzed to obtain their relative comparison:

- *S0*: current structure;
- *S1*: new structure with no filler (Fig. 7b);
- *S2*: new structure with *EPUMENT 140/5*-filled main basement (Fig. 7c);
- *S3*: new structure with *EPUMENT 140/5*-filled beam structure (Fig. 7d);
- *S4*: new structure with *EPUMENT 140/5*-filled basement and beam (Fig. 7e).

A numerical modal analysis was performed by means of the FEM software Ansys 17.1. All the components were modelled through 3D elements featuring quadratic shape functions (*Solid186*), with the exception of the basement feet that were meshed with finite elements based on the Timoshenko beam theory and featuring linear shape function (*Beam188*). Rigid fixed joints constrained the bottom nodes of these four elements to the ground.

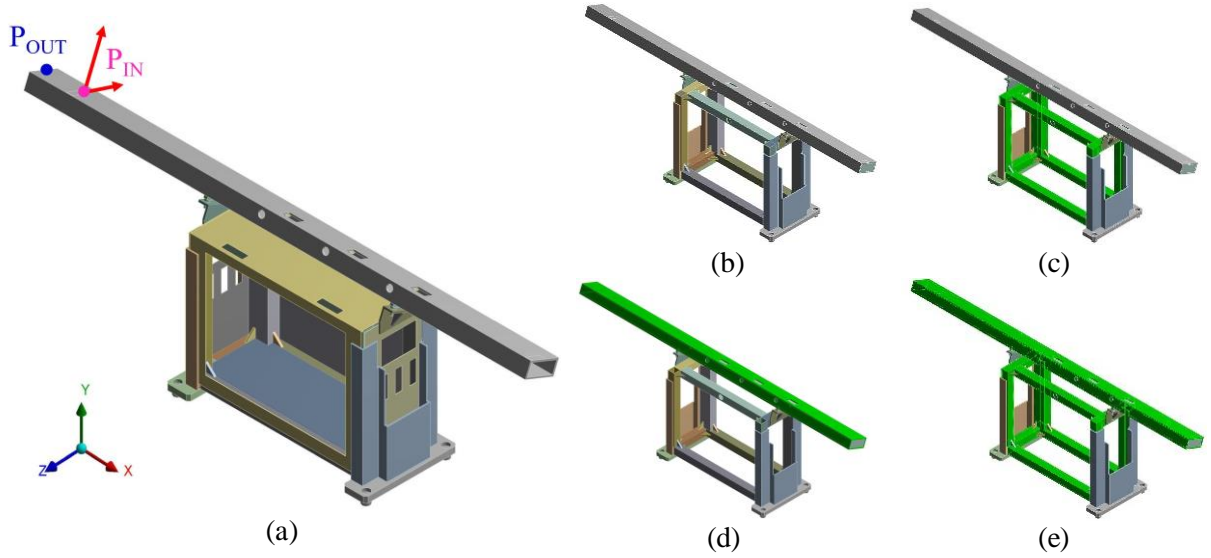


Figure 7. Design variants of new machine bed: (a) 3D model of *S1*, (b) *S1*, (c) *S2*, (d) *S3*, (e) *S4*.

Table 6: Natural frequencies of the machine bed design variants.

Model	Natural frequency ω_{ni} [Hz]							
<i>S0</i>	44	56	63	73	79	85	89	
<i>S1</i>	57	66	87	92	108	>125		
<i>S2</i>	59	68	87	96	108			
<i>S3</i>	46	54	72	77	93			
<i>S4</i>	48	56	73	81	95			

The mesh was controlled by imposing just one criterion on the automatic generation by the software, i.e. the setting the minimum number of elements (2 to 4) along the smallest size of the component geometries. The mesh convergence was studied on model *S1* and the resulting inference was then kept for all the other models. With two elements along the thickness of the thinnest components, a total of 25073 elements and 73801 nodes were generated. With four elements, instead, 59592 elements and 147928 nodes significantly increased the computational complexity of the model: nevertheless, no major benefits appeared in terms of accuracy, being only -0.5% the maximum variation of the natural frequency values.

Table 6 reports the natural frequencies (computed from the FEM models featuring two elements along the thickness of the smallest components), limited to the bandwidth 0–125 Hz, considered of interest for the machine working conditions. Local modes, e.g. the shell mode of a wall, are disregarded as they prove functionally negligible. The presence of hollow cross section beams instead of folded sheets makes the system stiffness increase: *S1* features natural frequencies higher than *S0* and, generally, altered mode shapes. On the other side, the additional mass of the polymer concrete filler, though apparently negligible for *S2*, tends to lower the natural frequencies of *S3* and *S4* with respect to *S1*.

In order to spot the filler influence on the machine dynamics in working conditions, forced vibration responses are computed simulating a rotating load due to the operational unit located inside the upper beam. With reference to Fig. 7(a) two sinusoidal forces, out-of-phase by 90° , are applied to point P_{IN} . Through harmonic analysis performed in the bandwidth 1–125 Hz, the acceleration response of the tip point P_{OUT} is analyzed in Frequency domain for all the design variants and used for a back-to-back comparison. Table 7 and Fig. 8 report the

RMS values and the Fourier Transform amplitudes of the *Y* and *Z* acceleration components, respectively. It is worth noting a few remarks:

- the new structure design, if empty (*S1*), worsens the machine bed dynamic behavior in operational conditions (Table 7), notwithstanding the natural frequency increments (Table 6, Fig. 8). This is due to the shape of the excited modes, which are different from *S0* ones and are apparently more critical;
- the presence of the damping material as a filler largely improves the vibration response with respect to *S1* (Table 7), even for the variant *S2* which features very similar natural frequencies (Table 6);
- both the design variants *S3* and *S4* outperform the other solutions, the filling of the upper beam with polymer concrete proving a successful expedient to damp vibrations.

Based on this analysis, solution *S3* is targeted as the most viable one, due to the limited complexity in the production process. In order to complete the overall feasibility study, a provisional cost analysis has been performed considering the polymer concrete cost (about 75 kg being required to fill the beam structure), the additional manpower effort (two persons working about one hour to prepare the mixture and fill the beam are estimated), and the possible increased cost for the design modifications of the new machine architecture (*S3*) with respect to the current version (*S0*). The latter can be considered basically negligible, due to the *assembly-to-order* business strategy of the Company and the actual production/sales volume

Table 7: *RMS* values of *Y* and *Z* acceleration components of point P_{OUT} .

	<i>S0</i>	<i>S1</i>	<i>S2</i>	<i>S3</i>	<i>S4</i>
a_{y_RMS} [m/s ²]	219.8	239.6	112.3	46.9	50.9
a_{z_RMS} [m/s ²]	151.8	249.2	69.6	49.4	47.6

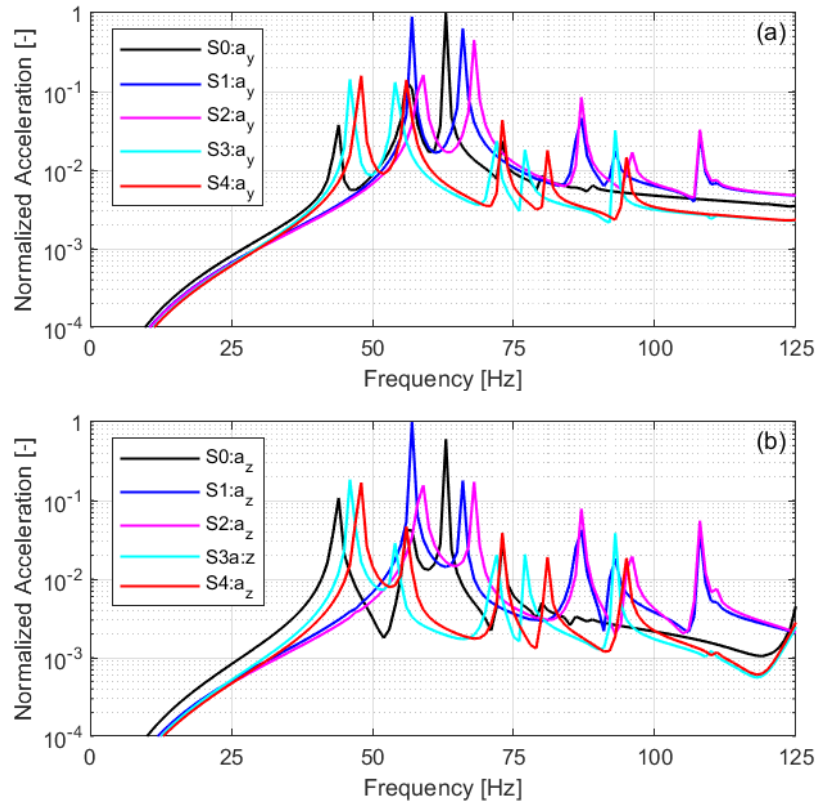


Figure 8. Fourier Transform normalized amplitudes of P_{OUT} acceleration *Y* and *Z* components.

of the machine over years. Other fixed costs, e.g. for modifications of the industrial plant possibly required, are unpredictable and thus disregarded at this stage. All in all, an increment of +6% has been evaluated for the production cost of the machine *S3* version with respect to the current one. It is worth noting that the case study is targeted on a low price-range model of a wider machines' family: if the design variant *S3* was implemented into the highest quality product, the estimated production cost increment would be limited to +0.5%.

Hence, starting from the preliminary version, further design modifications have been introduced to increase natural frequencies and – partly – alter the mode shapes, aiming to improve the system dynamic response. A prototype has been developed and subjected to a number of tests. Unfortunately, the final result is confidential and cannot be published: the above mentioned analysis is only reported with the purpose to illustrate the methodological approach.

5. CONCLUSION

The deep investigation on the damping properties of a commercial polymer concrete, to probe its potential use as a filler of an automatic machine bed, was the application-driven target of this study. The paper is mainly intended to illustrate the research approach. In particular, based on impact testing some quantitative metrics to evaluate the damping characteristics of the material are proposed in both the Time and Frequency domains. Moreover, starting from the experimentally determined modal parameters, alternative models of the material are determined and proposed for numerical analyses. Finally, as an example of practical application of the achieved findings, the design process to improve the dynamic response of the target machine is partly illustrated: the numerical results prove the actual effectiveness of the polymer concrete as a bed component filler to significantly damp the machine vibrations in working conditions.

ACKNOWLEDGMENTS

The authors gratefully acknowledge the funding by the Operational Programme of the European Regional Development Fund of the Emilia-Romagna Region (ROP-ERDF 2014-2020, DGR 887/2018).

REFERENCES

1. Altintas Y. *Manufacturing automation: metal cutting mechanics, machine tool vibrations, and CNC design*. Cambridge: Cambridge University Press, 2012.
2. Gegg BC, Suh CS and Luo ACJ. *Machine Tool Vibrations and Cutting Dynamics*. New York: Springer Science & Business Media, 2011.
3. Munoa J, Beudaert X, Dombovari Z, et al. Chatter suppression techniques in metal cutting. *CIRP Annals* 2016; 65(2):785–808.
4. Möhring HC, Brecher C, Abele E, et al. Materials in machine tool structures. *CIRP Annals* 2015; 64(2):725–748.
5. Bedi R, Chandra R and Singh SP. Reviewing some properties of polymer concrete. *Indian Concr J* 2014; 88(8):47–68.
6. Erbe T, Król J and Theska R. Mineral casting as material for machine base-frames of precision machines. *Univ.-Bibliothek* 2008.

-
7. Haddad H and Al Kobaisi M. Optimization of the polymer concrete used for manufacturing bases for precision tool machines. *Compos Part B-Eng* 2012; 43(8):3061-3068.
 8. Schulz H and Nicklau RG. Designing machine tool structures in polymer concrete. *Int J Cem Compos Lightweight Concr* 1983; 5(3):203-207.
 9. Weck M and Hartel R. Design, manufacture and testing of precision machines with essential polymer concrete components. *Precis. Eng.* 1985; 7(3):165-170.
 10. Cortés, F and Castillo G. Comparison between the dynamical properties of polymer concrete and grey cast iron for machine tool applications. *Mater. Des.* 2007; 28(5):1461-1466.
 11. Nabavi SF. Influence of polymers on concrete damping properties. In: *European conference of chemical engineering* (ed. WSEAS), Puerto De La Cruz, Tenerife, 30 November –2 December 2010, pp. 28–33.
 12. Orak S. Investigation of vibration damping on polymer concrete with polyester resin. *Cement Concrete Res* 2000; 30(2):171–174.
 13. Piratelli-Filho A and Levy-Neto F. Behavior of granite-epoxy composite beams subjected to mechanical vibrations. *Mater Res* 2010; 13(4):497–503.
 14. Vivek A, Holla V and Krupashankara MS. Polymer Concretes for Machine Tool Structures—A Review. *Int J Innov Res Sci Eng Technol* 2016; 5(10).
 15. Bruni C, Forcellese A, Gabrielli F, et al. Hard turning of an alloy steel on a machine tool with a polymer concrete bed. *J Mater Process Technol.* 2008; 202(1-3):493-499.
 16. Cho SK, Kim HJ and Chang SH. The application of polymer composites to the table-top machine tool components for higher stiffness and reduced weight. *Compos. Struct.* 2011; 93(2):492-501.
 17. Rahman M, Mansur MA, Lee LK, et al. Development of a polymer impregnated concrete damping carriage for linear guideways for machine tools. *Int J Mach Tools Manuf* 2001; 41(3):431–441.
 18. Suh JD and Lee DG. Design and manufacture of hybrid polymer concrete bed for high-speed CNC milling machine. *Int J Mech Mater Des* 2008; 4(2):113-121.
 19. Gade S and Herlufsen H. Digital Filter vs FFT techniques for damping measurements. *J Sound Vib* 1990; 24(3):24–32.
 20. Peeters B, Van der Auweraer H, Guillaume P, et al. The PolyMAX frequency-domain method: a new standard for modal parameter estimation?’, *Shock Vib* 2004; 11(3, 4):395–409.
 21. Ewins DJ, *Modal Testing: Theory, Practice and Application*. 2nd ed. Baldock: Research Studies Press Ltd., 2000.
 22. Schroeder MR. New method of measuring reverberation time. *J Acoust Soc Am* 1965; 37(6):1187–1188.
 23. Rao SS. *Mechanical Vibrations*. 5th ed., Upper Saddle River: Prentice Hall, 2004.
 24. Charney FA. Unintended consequences of modeling damping in structures. *J Struct Eng* 2008; 134(4):581–592.